Supplemental Information

Controlling for the Influence of Smoking and Psychiatric History on Resting State Functional Connectivity (RSFC)

The cocaine and control groups differed significantly in smoking and psychiatric history. To rule out their potential contribution to group differences in voxel-mirrored homotopic connectivity (VMHC), we performed two additional group-level analyses, which controlled for whether a participant (1) smoked; and (2) had a history of cannabis abuse/dependence, a history of alcohol abuse/dependence, and/or a history of any other psychiatric disorder.

Methods

To assess smoking status, we administered the Fagerstrom Test for Nicotine Dependence (FTND) (1). Unfortunately however, the FTND was not administered to all participants. Of the 7 cocaine-dependent participants (COC) who completed the Fagerstrom, 2 were non-smokers, and 4 had a total score of 0 and reported smoking 10 or fewer cigarettes per day. One participant had a score of 7 and reported smoking 31 or more cigarettes per day. For all other COC, their current smoking status was ascertained by reviewing their SCID interview. Of the 18 COC assessed in this way, 6 were determined to be smokers and 7 were currently non-smokers. Smoking status could not be determined for the remaining 5 participants.

Of the 16 control participants who completed the Fagerstrom, 3 were smokers. Two of the 3 reported smoking 10 or fewer cigarettes per day and one participant reported smoking 11-20 cigarettes per day.

In order to control for the potential effects of nicotine dependence on VMHC and RSFC, we repeated our analyses using "smoking status" as a covariate. We excluded all participants whose smoking status was unknown (5 COC, 8 controls). We then controlled for smoking status by modeling the number of cigarettes smoked per day as a covariate. The covariate was computed as follows: in those cases where the Fagerstrom was completed, we entered the maximum number of cigarettes for the band endorsed (i.e., if the participant reported

smoking 11-20 cigarettes per day, we covaried for 20). In those cases where the Fagerstrom was not available, we covaried for the number of cigarettes smoked per day, as reported during the SCID interview. In the two (cocaine-dependent) cases where that number was unknown, we entered the modal number (10 cigarettes per day) as the covariate.

We also repeated the VMHC and RSFC analyses in order to examine the effects of psychiatric history. Each analysis included 3 covariates that modeled whether a participant had (1) a history of cannabis abuse/dependence, (2) a history of alcohol abuse/dependence, and/or (3) a history of any other psychiatric disorder. For each covariate, a positive history was indicated with 1, and a negative history with a 0.

Results

As shown in Figures S3 and S4, and reported in Table S1, group differences in both VMHC and seed-based RSFC were largely unaffected when smoking status and psychiatric history were taken into account, suggesting that the group differences in VMHC and RSFC are not likely to be attributable to differences in cigarette smoking or psychiatric history.

Voxel-Based Morphometry (VBM)

VBM Analysis

In order to mitigate concerns that between-group differences in interhemispheric structural asymmetry could drive the observed group differences in VMHC, we used FSL's VBM-style analysis pipeline (2,3) to compute gray matter (GM) volume measures for each participant.

Each participant's high-resolution anatomical image was skull-stripped to remove non-brain material, and segmented into GM, white matter and cerebrospinal fluid. The resultant GM images were registered to the ICBM152 gray matter template (included with FSL) with 2 x 2 x 2 mm resolution, using a 12 degrees-of-freedom affine registration (*FLIRT*). These images were then averaged together with their mirror images, in order to create a

symmetric study-specific GM template. Each individual's native GM image was then registered to this study-specific GM template using FNIRT nonlinear registration, and each voxel was subsequently divided by the Jacobian of the nonlinear warp field (2) in order to compensate ("modulate") for contraction or enlargement caused by the non-linear transformation. The modulated normalized GM images were then smoothed with an isotropic Gaussian kernel with a sigma of 3 mm (<7 mm FWHM).

We tested for the presence of group differences in GM across the entire brain, as well as group differences in GM asymmetries (i.e., left-right differences in GM volume).

To test for regional group differences in GM volume, the modulated normalized GM images were entered into a voxel-wise non-parametric group analysis, performed using the FSL program *randomize*. Five thousand permutations were performed. Age and sex were modeled as nuisance covariates. Voxel-wise statistics were corrected for multiple comparisons (at $p < 0.05$) using threshold-free cluster enhancement (TFCE). In a secondary, exploratory analysis, we also performed a parametric (t-test) group comparison, with false discovery rate (FDR) correction for multiple comparisons ($q < 0.05$).

In order to quantify left-right (L-R) differences in GM volume, we computed a structural variant of VMHC, named voxel-mirrored homotopic morphometry (VMHM; see Zuo *et al*., (4) for the first application of this measure). Zuo *et al.* defined VMHM as

$$\mathrm{VMHM} = 1 - \frac{\left|\mathrm{L}_{GM} - \mathrm{R}_{GM}\right|}{\mathrm{L}_{GM} + \mathrm{R}_{GM}}$$

where L_{GM} and R_{GM} are the gray matter morphometry measures for each voxel within the left and right hemispheres, respectively.

We tested for the presence of global and regional group differences in VMHM. To test for global differences in VMHM, we first averaged VMHM values across all brain voxels within a unilateral hemispheric gray matter mask (as there is only one VMHM value for each pair

of homotopic voxels). The mask was created as the conjunction between a unilateral mask created using the MNI152 gray matter tissue prior included with FSL, thresholded at 25% tissue-type probability and the mean (across all participants) GM image. The group comparison of global VMHM was performed using a t-test, after regressing out the effects of age and sex from the VMHM values.

To test for regional group differences in VMHM, individual VMHM images were entered into a voxel-wise non-parametric group comparison, performed using the FSL program *randomize*. The unilateral mean GM image was used as a mask and 5000 permutations were performed. Age and sex were modeled as nuisance covariates. Voxel-wise statistics were corrected for multiple comparisons (at $p < 0.05$) using TFCE.

Controlling for L-R GM differences (VMHM) in the VMHC Analysis

We controlled for the effects of L-R differences in GM on group differences (as quantified by VMHM) in VMHC by repeating the primary VMHC analysis, and including each participant's 3-D VMHM volume as a voxel-dependent covariate.

Results

Voxel-wise group comparisons of whole-brain GM volume did not reveal any significant group differences (using either parametric or non-parametric analyses), nor did voxel-wise group comparisons of VMHM. There were no significant group differences in global GM or VMHM measures, nor was there a significant group difference in mean VMHM within the inferior frontal sulcus (IFS) area exhibiting significant group differences in the primary VMHC analysis.

Figure S3C shows the group-level VMHC for the control and cocaine-dependent groups and significant group differences in VMHC ($Z > 2.3$, cluster-level $p < 0.05$, corrected) when the voxel-dependent VMHM covariate was included in the group-level analysis (see also Table S1). The area exhibiting significant group differences was reduced only slightly, relative to the primary analysis (i.e., Figure 1C).

Within-Sample Replication Analyses

A second resting state scan from the same session was available for 19 of the 25 COC and for 21 of the 24 control participants, allowing us to test whether group differences in VMHC and seed-based RSFC analyses were stable across two resting state scans collected <1 hour apart. The secondary scan data was also used to plot group differences in VMHC and seed-based RSFC, in recognition of the fact that non-independence in voxel-wise analyses of group differences necessarily provides inflated estimates of effect sizes (5-7).

The secondary scan data were processed in the same manner as the primary scan data. Cross-scan consistency was assessed by creating a functional mask for each area exhibiting significant group differences in the primary analyses, and extracting VMHC and RSFC values from each participant's respective secondary scan data. Pearson correlations were computed to quantify the consistency of VMHC and RSFC scores. Confirmatory group comparisons were performed using t-tests, controlling for age, sex and whether the participants' eyes were open or closed (12 of the control participants' secondary scans were "eyes-closed" scans).

Within-Sample Replication Results

Consistent with Shehzad *et al.* (8), we observed good within-session consistency for VMHC and seed-based RSFC across the two scans. Figure 1B shows the results of the within-sample VMHC replication analysis. VMHC values across the IFS area exhibiting significant group differences in the primary VMHC analysis (i.e., shown in Figure 1C) were highly consistent across scans (controls: $r = 0.495$, $p < 0.05$; COC: $r = 0.587$, $p < 0.01$; all participants: $r = 0.69$; $p < 0.0001$), and the group difference in VMHC within the IFS remained highly significant in the secondary scan data (Figure 1D; controls mean Scan 2 VMHC = 0.38 ± 0.10, COC mean Scan 2 VMHC = 0.26 ± 0.09; $t(2,38) = 4.13$, $p < 0.001$).

Figure S2 shows the results of the within-sample seed-based RSFC replication analysis. RSFC values across the frontal and parietal areas exhibiting significant group differences in RSFC with the right and left IFS seeds (i.e., the areas shown in the right-most panel of

Figure S1) were consistent across scans, although, within each group, the correlation between the left IFS seed and with right IFS appeared to be less robust than the other connections (Figure S2A - left IFS seed to right prefrontal cortex: controls: r = 0.32, p = 0.16; COC: r = 0.35, p = 0.11; all participants: r = 0.42; $p < 0.01$; Figure S2B - left IFS seed to right intraparietal sulcus (IPS): controls: r = 0.52, $p < 0.05$; COC: r = 0.54, $p < 0.05$; all participants: r = 0.65; $p < 0.0001$; Figure S2C - right IFS seed to left prefrontal cortex: controls: r = 0.56, $p < 0.01$; COC: r = 0.46, $p < 0.05$; all participants: r = 0.65; $p < 0.0001$). Further, group differences for all but one connection remained significant in the secondary scan data, while the group difference for RSFC between the left IFS seed and right PFC just escaped significance (Figure S2D – left IFS seed to right prefrontal cortex: controls mean Scan 2 RSFC = 0.213 $\pm$ 0.13, COC mean Scan 2 VMHC = 0.14 $\pm$ 0.11; t(2,38) = 1.8261, p = 0.0753; Figure S2E – left IFS seed to right IPS: controls mean Scan 2 RSFC = 0.271 $\pm$ 0.08, COC mean Scan 2 VMHC = 0.187 $\pm$ 0.08; t(2,38) = 3.182, $p < 0.005$; Figure S2F – right IFS seed: controls mean Scan 2 RSFC = 0.378 $\pm$ 0.11, COC mean Scan 2 VMHC = 0.282 $\pm$ 0.09; t(2,38) = 3.06, $p < 0.005$).

Diffusion Tensor Imaging (DTI)

DTI Analyses

In addition to the primary voxel-wise non-parametric group comparisons of DTI fractional anisotropy (FA), we performed a series of secondary, exploratory, parametric voxel-wise analysis, in which we tested for group differences in (non-skeletonized) FA, first diffusion eigenvalue (L1), mean diffusivity (MD) and radial diffusivity (RD) values using group-level voxel-wise t-test analyses (mixed-effects ordinary least squares), covarying for age and sex. FDR correction for multiple comparisons ($q < 0.05$) was applied.

We also examined the relationship between FA and reported duration of cocaine use, reported duration of dependence (retroactively calculated on the basis of the SCID) and Cognitive Failures Questionnaire (CFQ) scores within the cocaine group. A covariate modeling each of these measures for each participant was entered in (1) a voxel-wise non-parametric group comparison, performed using the FSL program *randomize* and corrected

for multiple comparisons (at $p < 0.05$) using TFCE; and (2) a parametric (t-test) group comparison, covarying for age and sex, with FDR correction for multiple comparisons ($q < 0.05$).

Finally, we performed an ROI-based analysis of specific white matter tracts (using the Jülich atlas (9) available as part of FSL) to test for group-differences in FA (skeletonized and non-skeletonized). For each white matter tract ROI included in the Jülich atlas, we averaged FA values across all voxels falling within that ROI for each participant. We then used t-tests to perform group comparisons, controlling for age, sex and scan order. Finally, we also tested for correlations between FA within each of these white matter tract ROIs and mean VMHC within an ROI comprising the IFS area exhibiting significant group differences in the primary VMHC analysis.

DTI Results

As is reported in the main text, voxel-wise non-parametric group comparisons of the skeletonized FA data revealed no significant group differences. No significant group differences were evident when age and sex covariates were removed from the analysis; when spatial non-stationarity was controlled for; nor when a parametric voxel-wise analysis of all (i.e., non-skeletonized) white matter FA, L1, MD and RD values was performed.

The ROI-based analysis of specific white matter tracts similarly did not reveal any significant group differences in FA. In addition, no significant correlations between FA and VMHC were observed.

In the secondary exploratory analyses, we observed a significant positive relationship between the reported duration of cocaine dependence and FA in the right posterior limb of the internal capsule (using non-parametric testing in *randomize* and TFCE correction for multiple comparisons), and between duration of dependence and FA in the posterior limb of the internal capsule bilaterally using a less conservative parametric voxel-wise approach and FDR correction for multiple comparisons (Figure S5).

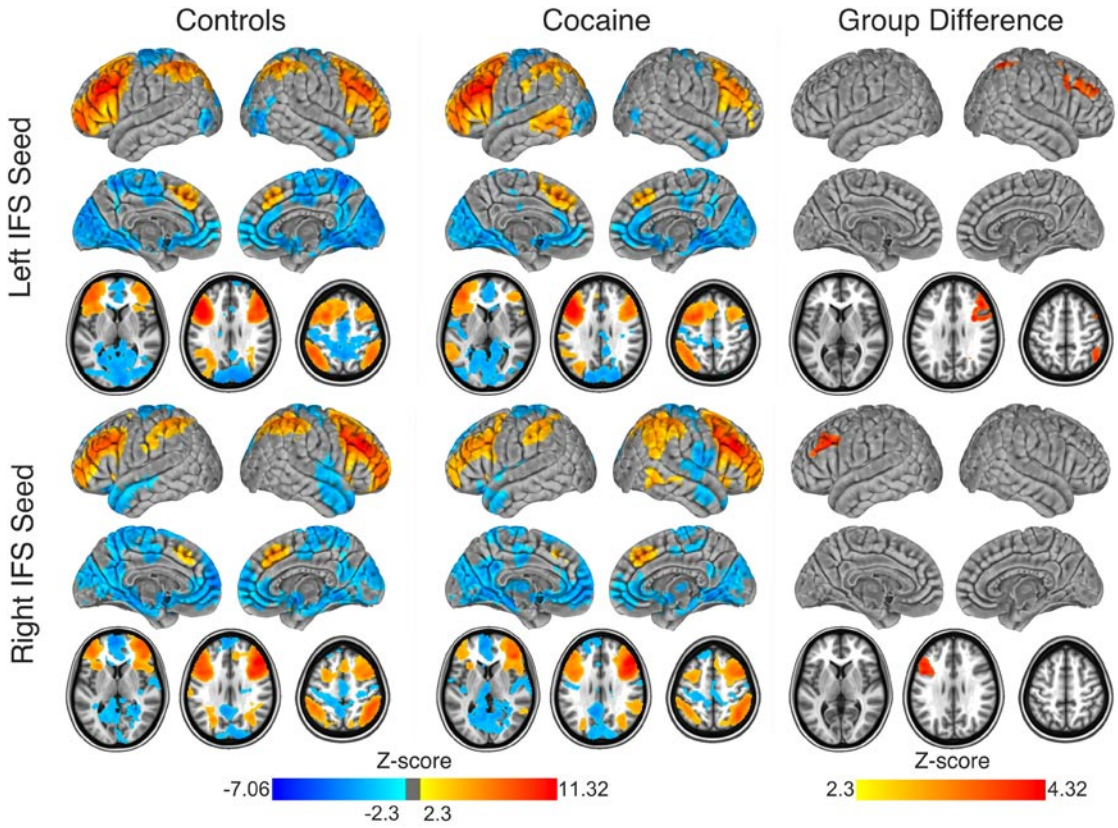

Figure S1. Seed-based resting state functional connectivity (RSFC) for left and right inferior frontal sulcus (IFS) seeds. Left and right IFS seeds exhibited RSFC with a large dorsal fronto-parietal network comprising lateral prefrontal cortex, pre-supplementary motor area (preSMA), posterior parietal cortex and intraparietal sulcus (IPS), posterior middle temporal cortex, and the caudate. Direct voxel-wise group contrasts revealed stronger RSFC between the right IFS and contralateral (left) IFS and middle frontal gyrus (MFG), and between the left IFS seed and contralateral (right) IFS, MFG, dorsal premotor, and IPS, in the controls, relative to the cocaine-dependent group. Axial slices (z = 5; 28; and 51) are displayed according to neurological convention (right is right).

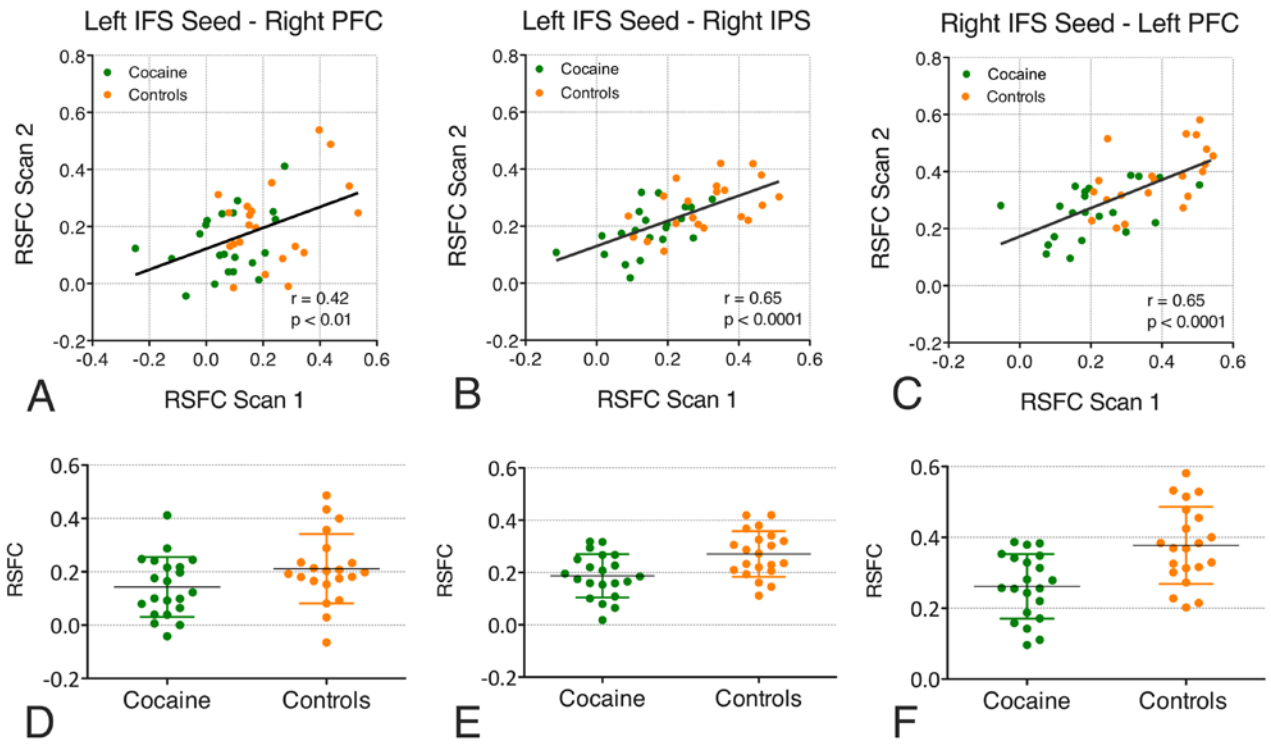

Figure S2. Cross-scan consistency of resting state functional connectivity (RSFC) and group differences.

A. Cross-scan consistency of mean RSFC values between the left inferior frontal sulcus (IFS) seed and the right IFS/ middle frontal gyrus (MFG) area exhibiting significant group differences in the primary RSFC analysis (i.e., the areas shown in the top right section of Figure S1; controls: r = 0.32, $p = 0.16$; cocaine: r = 0.35, $p = 0.11$; all participants: r = 0.42; $p < 0.01$). See supplemental text, above, for full details of the within-sample replication analysis.

B. Cross-scan consistency of mean RSFC values between the left IFS seed and the intraparietal sulcus (IPS) area exhibiting significant group differences in the primary RSFC analysis (left IFS seed to right IPS: controls: r = 0.52, $p < 0.05$; cocaine: r = 0.54, $p < 0.05$; all participants: r = 0.65; $p < 0.0001$). See supplemental text, above, for full details of the within-sample replication analysis.

C. Cross-scan consistency of mean RSFC values between the right IFS seed and the left IFS/MFG exhibiting significant group differences in the primary RSFC analysis (i.e., the areas shown in the bottom right section of Figure S1; controls: r = 0.56, $p < 0.01$; cocaine: r = 0.46, $p < 0.05$; all participants: r = 0.65; $p < 0.0001$).

D. Mean RSFC values within the right IFS/MFG area exhibiting significant group differences in RSFC with the left IFS seed are plotted for the secondary scan (Scan 2) data. The group difference in RSFC for the secondary scan just escapes significance (controls mean Scan 2 RSFC = 0.213 ± 0.13, cocaine mean Scan 2 VMHC = 0.14 ± 0.11; t(2,38) = 1.8261, $p = 0.0753$).

E. Mean RSFC values within the right IPS area exhibiting significant group differences in RSFC with the left IFS seed are plotted for the secondary scan (Scan 2) data. The group

difference in RSFC for the secondary scan is significant (controls mean Scan 2 RSFC = 0.271 ± 0.08, cocaine mean Scan 2 VMHC = 0.187 ± 0.08; t(2,38) = 3.182, $p < 0.005$).
F. Mean RSFC values across the left IFS/MFG area exhibiting significant group differences in RSFC with the right IFS seed are plotted for the secondary scan (Scan 2) data. The group difference in RSFC for the secondary scan is significant (controls mean Scan 2 RSFC = 0.271 ± 0.08, cocaine mean Scan 2 VMHC = 0.187 ± 0.08; t(2,38) = 3.182, $p < 0.005$).

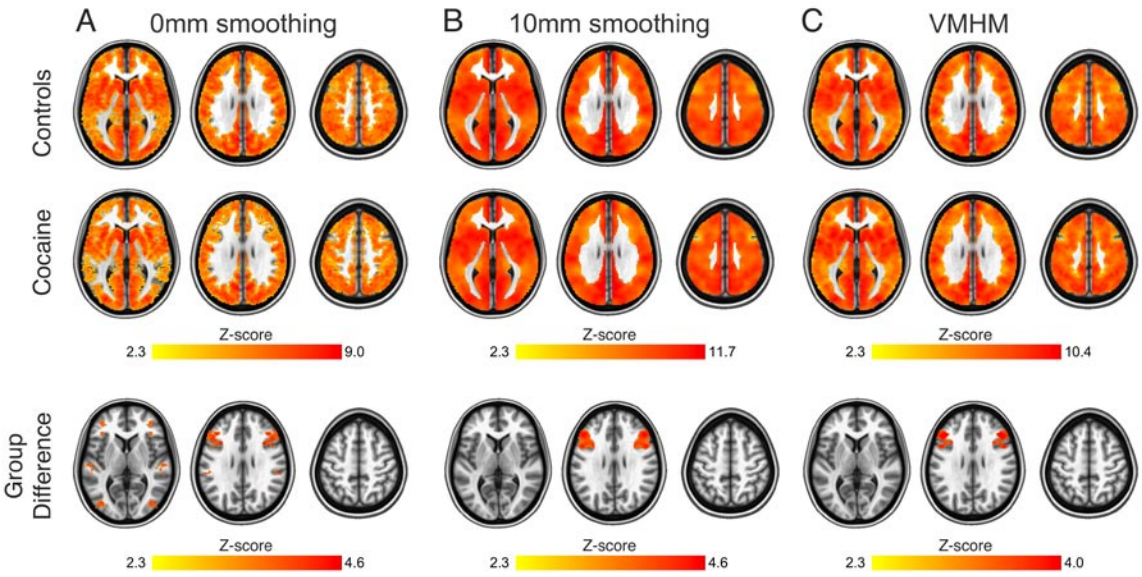

Figure S3. Supplementary analyses of voxel-mirrored homotopic connectivity (VMHC).
A. Group-level VMHC for the control and cocaine-dependent groups (upper panels) and significant group differences in VMHC (lower panel; Z > 2.3, cluster-level $p < 0.05$, corrected) when no smoothing (0 mm) was applied during preprocessing. In addition to group differences in the same inferior frontal sulcus (IFS) region observed in the primary analysis, group differences in VMHC were also evident in superior temporal cortex, anterior supramarginal gyrus, and lateral occipital cortex.
B. Group-level VMHC for the control and cocaine-dependent groups (upper panels) and significant group differences in VMHC (lower panel; Z > 2.3, cluster-level $p < 0.05$, corrected) when extensive smoothing (10 mm FWHM) was applied during preprocessing. The spatial extent of the area exhibiting significant group differences was enlarged, but encompassed the same regions as in the primary analysis (i.e., Figure 1C).
C. Group-level VMHC for the control and cocaine-dependent groups (upper panels) and significant group differences in VMHC (lower panel; Z > 2.3, cluster-level $p < 0.05$, corrected) when a voxel-dependent covariate quantifying left-right differences in grey matter volume (i.e., VMHM see supplemental text, above, for further details) was included in the group-level analysis. The area exhibiting significant group differences was reduced only slightly, relative to the primary analysis (i.e., Figure 1C).

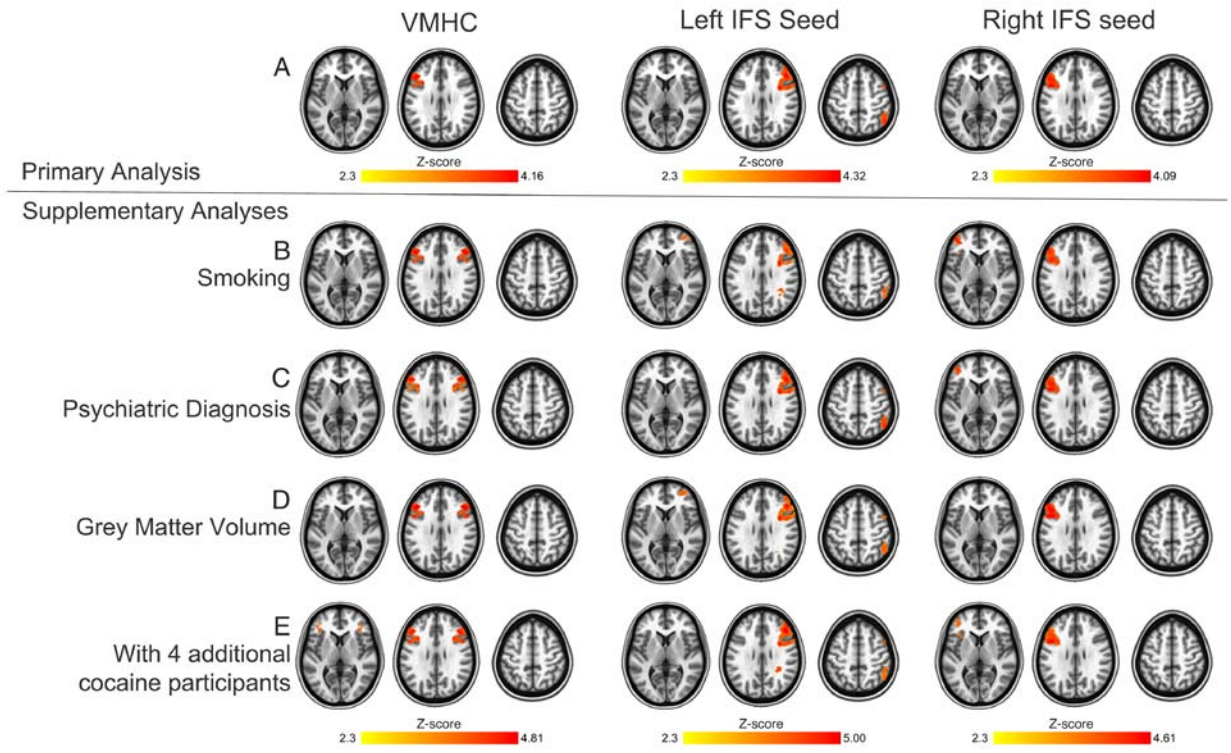

Figure S4. Supplementary analyses of voxel-mirrored homotopic connectivity (VMHC) and seed-based resting state functional connectivity (RSFC).
A. Significant group differences in VMHC and seed-based RSFC observed in the primary analyses (i.e., as shown in Figures 1 and S1).
B. Significant group differences in VMHC and seed-based RSFC when a covariate modeling the number of cigarettes smoked per day was included in the group-level analysis (excluding participants whose smoking status was unknown (5 cocaine-dependent participants, 8 controls)).
C. Significant group differences in VMHC and seed-based RSFC when covariates modeling whether a participant had a history of cannabis abuse/dependence, alcohol abuse/dependence and/or any other psychiatric disorder were included in the group-level analysis.
D. Significant group differences in VMHC and seed-based RSFC when a voxel-dependent covariates quantifying VMHM (for the VMHC analysis only – this is the same image as shown in Figure S3C) or whole-brain gray matter volume (for the seed-based analyses) were included in the group-level analyses.
E. Significant group differences in VMHC and seed-based RSFC when all 29 cocaine-dependent participants (mean age 37.27 ± 9 years) were included in the group-level analysis and compared with the 24 controls.
In all of the supplementary analyses of VMHC and seed-based RSFC, group differences were basically unchanged, relative to the primary analysis **(A)**, suggesting that these potentially confounding factors do not explain the group differences in VMHC and seed-based RSFC.

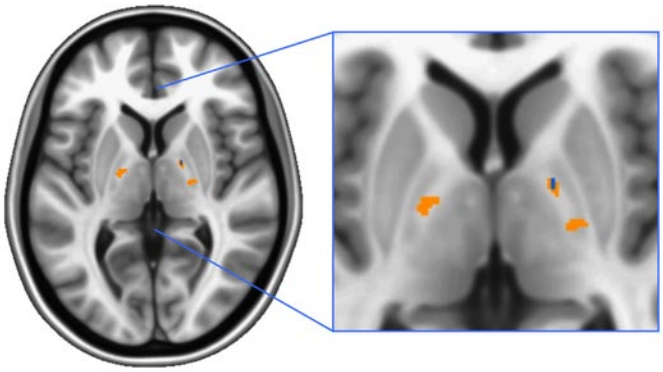

Figure S5. Significant correlation between diffusion tensor imaging (DTI) fractional anisotropy (FA) and reported duration of dependence.
In an exploratory analysis, we examined the relationship between FA and reported duration of cocaine dependence (years; retroactively calculated on the basis of the SCID). Using non-parametric testing in *randomize,* and threshold-free cluster enhancement correction for multiple comparisons ($p < 0.05$, corrected), we observed a significant positive relationship between the reported duration of dependence and FA in the right posterior limb of the internal capsule (shown in blue). Using a less conservative parametric voxel-wise approach, and false discovery rate (FDR) correction for multiple comparisons ($q < 0.05$), FA in a more extensive, bilateral portion of the posterior limb of the internal capsule was significantly positively correlated with duration of dependence (shown in orange).

Table S1. Significant group differences in VMHC in the supplementary analyses (i.e., shown in Figures S3 and S4). All regions listed showed significantly greater VMHC in the control group, relative to the cocaine group.

	Peak (MNI)			Cluster Size	
Cluster Location	**x**	**y**	**z**	**(2 mm³ voxels)**	**Peak Z**
0 mm Smoothing (Figure S3A)					
IFS, MFG	±34	16	28	550	8.53
Lateral occipital cortex	±42	-82	8	159	4.55
Supramarginal gyrus	±58	-32	32	130	3.89
Superior temporal gyrus	±56	-28	4	130	3.77
Inferior frontal gyrus	±40	48	-6	116	3.92
10 mm Smoothing (Figure S3B)					
IFS, MFG, IFG, ventral PCG	±50	10	32	986	4.46
Controlling for Voxel-wise L-R Gray Matter Differences (VMHM; Figure S3C/S4D)					
IFS, MFG, IFG, ventral PCG	±42	28	28	470	3.89
Controlling for Smoking (Figure S4B)					
IFS, MFG, IFG, ventral PCG	±42	10	32	654	4.28
Controlling for Psychiatric Diagnosis (Figure S4C)					
IFS, MFG, IFG, ventral PCG	±50	10	32	496	4.15
Comparing 29 Cocaine and 24 Controls (Figure S4E)					
IFS, MFG, IFG, ventral PCG	±50	10	30	696	4.72

IFG, inferior frontal gyrus; IFS, inferior frontal sulcus; MFG, middle frontal gyrus; MNI, Montreal Neurological Institute; PCG, precentral gyrus; VMHC, voxel-mirrored homotopic connectivity; VMHM, voxel-mirrored homotopic morphometry.

Table S2. Significant group differences in seed-based RSFC in the supplementary analyses. All regions listed showed significantly greater RSFC in the control group, relative to the cocaine group.

Cluster Location	Peak (MNI) x	y	z	Cluster Size (2 mm^3 voxels)	Peak Z
Controlling for Smoking (Figure S4B)					
Left IFS Seed					
Right IFS, MFG, IFG, ventral PCG	32	8	30	1387	3.27
Right Intraparietal Sulcus, Posterior Superior Parietal Cortex	44	-40	36	799	3.77
Right IFG	42	48	-4	678	4.26
Right IFS Seed					
Left IFS, MFG, IFG	-42	34	14	1666	4.48
Controlling for Psychiatric Diagnosis (Figure S4C)					
Left IFS Seed					
IFS, MFG, IFG, ventral PCG	46	30	26	1823	4.18
Intraparietal Sulcus, Posterior Superior Parietal Cortex	52	-56	52	708	4.28
Right IFS Seed					
Left IFS, MFG, IFG	-44	32	20	1625	4.03
Controlling for VMHM (VMHC analysis) or Voxel-wise Gray Matter Volume (Seed-based analysis; Figure S4D)					
Left IFS Seed					
IFS, MFG, IFG, ventral PCG	46	30	26	1801	4.44
Intraparietal Sulcus, Posterior Superior Parietal Cortex	52	-56	52	784	4.06
Right IFG	36	48	-4	644	4.48
Right IFS Seed					
Left IFS, MFG, IFG	-50	12	32	1219	3.83
Comparing 29 Cocaine and 24 Controls (*Figure S4E)*					
Left IFS Seed					
IFS, MFG, IFG, ventral PCG	46	30	28	1996	4.42
Intraparietal Sulcus, Posterior Superior Parietal Cortex	28	-44	30	724	4.02
Right IFS Seed					
Left IFS, MFG, IFG	-44	32	20	1959	4.61

IFG, inferior frontal gyrus; IFS, inferior frontal sulcus; MFG, middle frontal gyrus; MNI, Montreal Neurological Institute; PCG, precentral gyrus; VMHC, voxel-mirrored homotopic connectivity; VMHM, voxel-mirrored homotopic morphometry.

Table S3. Centers of spherical regions of interest for 16 core nodes (8 in each hemisphere) of the dorsal attention network (DAN).

	Center (MNI)		
	x	**y**	**z**
Anterior Inferior Frontal Sulcus (antIFS)	±40	48	-2
Middle IFS (midIFS)	±46	30	24
Posterior IFS (postIFS)	±44	12	30
Frontal Eye Fields (FEF)	±40	-48	42
Intraparietal Sulcus (IPS)	±34	8	60
Middle Temporal Area (MT)	±54	-48	-6
Presupplementary Motor Area (preSMA)	±6	26	44
Caudate	±12	8	-8

Supplemental References

1. Heatherton TF, Kozlowski LT, Frecker RC, Fagerstrom KO (1991): The Fagerstrom Test for Nicotine Dependence: a revision of the Fagerstrom Tolerance Questionnaire. *Br J Addict*. 86:1119-1127.
2. Good CD, Johnsrude IS, Ashburner J, Henson RN, Friston KJ, Frackowiak RS (2001): A voxel-based morphometric study of ageing in 465 normal adult human brains. *Neuroimage*. 14:21-36.
3. Zhang Y, Brady M, Smith S (2001): Segmentation of brain MR images through a hidden Markov random field model and the expectation-maximization algorithm. *IEEE Trans Med Imaging*. 20:45-57.
4. Zuo XN, Kelly C, Di Martino A, Mennes M, Margulies DS, Bangaru S, *et al.* (2010): Growing together and growing apart: Regional and sex differences in the lifespan developmental trajectories of functional homotopy. *J Neurosci*. 30:15034-15043.
5. Kriegeskorte N, Simmons WK, Bellgowan PS, Baker CI (2009): Circular analysis in systems neuroscience: the dangers of double dipping. *Nat Neurosci*. 12:535-540.
6. Vul E, Harris C, Winkielman P, Pashler H (2009): Puzzlingly high correlations in fMRI studies of emotion, personality and social cognition. *Perspect Psychol Sci* 4:274-290.
7. Poldrack RA, Mumford JA (2009): Independence in ROI analysis: where is the voodoo? *Soc Cogn Affect Neurosci*. 4:208-213.
8. Shehzad Z, Kelly AM, Reiss PT, Gee DG, Gotimer K, Uddin LQ, *et al.* (2009): The resting brain: unconstrained yet reliable. *Cereb Cortex*. 19:2209-2229.
9. Eickhoff SB, Stephan KE, Mohlberg H, Grefkes C, Fink GR, Amunts K, *et al.* (2005): A new SPM toolbox for combining probabilistic cytoarchitectonic maps and functional imaging data. *Neuroimage*. 25:1325-1335.